Local backscattering in the quantum Hall regime

S. Kičin, A. Pioda, T. Ihn,* and K. Ensslin
Solid State Physics Laboratory, ETH Zurich, 8093 Zurich, Switzerland

D. C. Driscoll and A. C. Gossard
Materials Department, University of California, Santa Barbara, California, USA
(Received 7 April 2004; published 3 November 2004)

A two-dimensional electron gas in the quantum Hall regime has been investigated by tuning the local potential with the metallic tip of a scanning force microscope. The longitudinal four-terminal resistance of the Hall bar structure was recorded while the tip was scanned above. The resulting resistance images exhibit local features that show a $1/B$-periodicity. These features line up along the Hall bar edges resembling the formation of edge channels. At certain filling factors they develop a subtle fine structure indicating the intricate microscopic variations of states in real space.

DOI: 10.1103/PhysRevB.70.205302 PACS number(s): 73.43.−f

I. INTRODUCTION

The quantum Hall effect[1] (QHE) is one of the unique and fundamental phenomena occurring in two-dimensional electron gases (2DEGs) at low temperatures. Its discovery initiated a tremendous amount of experimental and theoretical research.[2–4] One of its most remarkable properties is the precision of the quantization irrespective of the material and its quality which allows to utilize the effect as a resistance standard.[5] A key ingredient for the understanding of the QHE is the localization of states in the tails of the Landau levels in high magnetic fields and the existence of extended states at sample boundaries or internal edges. These edge states can be described self-consistently and the formation of compressible and incompressible stripes of integer filling factors have been predicted.[6,7] The existence of extended states with a transmission of one between neighboring sample contacts is the basis for the description of the QHE in the framework of the Landauer-Büttiker theory of linear transport.[8] It has been checked, for example, with measurements where stripe gates across a Hall bar sample were used for selective backscattering of edge states.[9] Although this model supplies a very intuitive and transparent picture of the effect, it does not settle the question, where the current flows in the bulk of a sample and how the current density pattern changes with varying magnetic field.

As a consequence, many attempts have been made to measure the internal structure of the electron gas in the QHE-regime with local probes. Early experiments used the electron-phonon interaction[10] or optical techniques with a spatial resolution down to 1 μm.[11–13] Later it was tried to detect edge channels inductively.[14,15] Recently, edge channels were imaged with a metallic single-electron transistor fabricated near the edge of a 2DEG.[16] Scanning probe techniques with their unprecedented potential of spatial resolution have also been employed for the local investigation of 2DEGs in the QHE-regime during the past few years. Among them are measurements with a scanning single-electron transistor,[17,18] experiments using scanned potential microscopy,[19] Kelvin probe techniques,[20–22] subsurface charge accumulation,[23–25] and tunnelling between edge channels.[26,27]

In this paper we follow the route of applying scanning probe techniques to a 2DEG in the QHE-regime. In our measurements we use the conducting tip of a scanning force microscope as a local gate and measure its influence on the longitudinal and Hall resistances at a temperature of 300 mK. The method is known as the scanning gate technique which has found a number of applications at zero magnetic field.[28–34] In the QHE-regime the tip-induced potential changes the microscopic potential landscape in the bulk of the sample locally. Here, we focus on the longitudinal resistance. We find that local backscattering between opposite edges of the sample can be enhanced or diminished depending on tip position and magnetic field. The tip-induced backscattering can be mapped out at constant magnetic field by analyzing the longitudinal resistance of the sample. The tip is found to have the strongest influence on the resistance between even filling factors (in cases where the spin splitting is not resolved), where extended states exist in the bulk of the structures. Similar resistance patterns occur in a $1/B$-periodic fashion. Striking features appear in the images that are lined up along the sample edges. These features can have remarkable capillary fine structure on length scales of about 200 nm. The Hall resistance is found to be very robust against the tip-induced potential on quantum Hall plateaus and sensitive in transition regions between them.

II. SAMPLES AND MEASUREMENT SETUP

Bar shaped samples with a width of 4 μm and a length of 10 μm between longitudinal voltage probes have been fabricated on the basis of a shallow Ga[Al]As heterostructure confining a 2DEG 34 nm below the sample surface. A back gate electrode made of highly doped GaAs is situated 1.3 μm below the 2DEG and isolated with a layer of ErAs islands in between.[35] The electron density in the 2DEG at zero back gate voltage was $n_s = 5.5 \times 10^{15}\ \mathrm{m}^{-2}$, the mobility $\mu = 8.5\ \mathrm{m}^2/\mathrm{V\,s}$ as determined from Hall and Shubnikov-de Haas measurements performed at a temperature of 300 mK. These values correspond to a mean free path of 1 μm ensuring that electron transport is diffusive on the length scales of the structure.

 ©2004 The American Physical Society

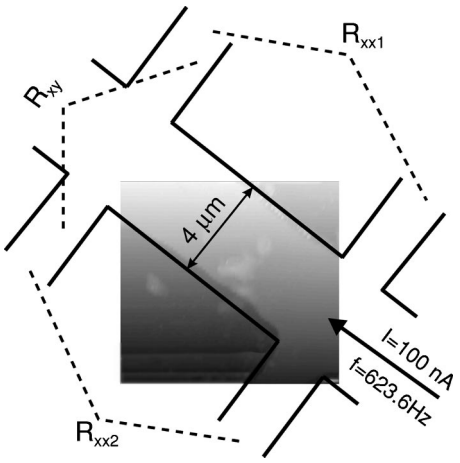

FIG. 1. Topography scan of the Hall bar taken at 300 mK. The solid lines indicate the mesa edges of the Hall bar including four voltage probes. A constant current $I=100$ nA is driven along the Hall bar axis at a frequency of 623.6 Hz.

The measurements were carried out using a homebuilt scanning force microscope operating at 300 mK in a ^{3}He-cryostat.[36] Magnetic fields up to 9 T can be applied normal to the plane of the 2DEG. The scan range is 8.8 μm $\times$ 8.8 μm at base temperature. Piezoelectric tuning fork sensors[37–39] are employed for controlling the distance of the conducting tip above the sample surface in dynamic mode. A phase locked loop is used for measuring shifts of the sensor's resonance frequency with a relative accuracy better than 10^{-7}. Details about these sensors and the phase-locked loop can be found in Refs. 36 and 39–41. The conductive PtIr tip attached to the tuning fork sensor can either be connected to an external voltage source or to a current-voltage converter. It couples capacitively to the 2DEG.

The measured frequency shift of the tuning fork resonator, Δf, is proportional to the force gradient, F', acting on the tip. The force gradient is related to the voltage U applied between the tip and the 2DEG via[36,42]

$$\Delta f \propto F' \propto C''(U - U_{\mathrm{CPD}})^2 \tag{1}$$

with C'' being the second derivative of the tip-sample capacitance and U_{CPD} being the (local) contact potential difference between the tip and the sample surface. Two scan modes have been employed in the course of the experiments presented here. In the usual scan mode the z-feedback operates at constant frequency shift Δf. An example of an image of the Hall bar taken at 300 mK is shown in Fig. 1. The overlaid solid lines indicate the mesa edges of the structure with the four voltage probes. Alternatively we can scan in constant height mode in which the feedback is switched off and the tip is bound to a plane parallel to the sample surface. In this imaging mode we can, for example, map the frequency shift Δf as a function of lateral tip position (x,y) for fixed tip-sample voltage U. According to Eq. (1) the frequency shift is sensitive to the local capacitance derivative $C''(x,y)$ and the local contact potential difference $U_{\mathrm{CPD}}(x,y)$. An

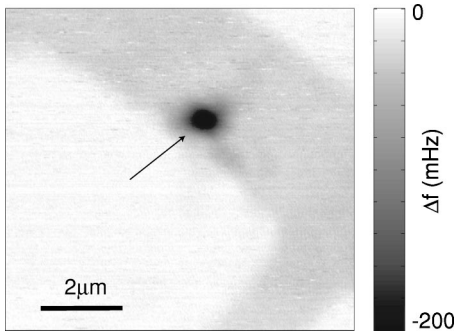

FIG. 2. Constant height scan of the Hall bar taken at 300 mK. The tip sample voltage was $U=-4$ V, the height above the Hall bar mesa was 85 nm. The gray scale represents the frequency shift Δf of the tuning fork resonance. The arrow points to a charged spot on the surface.

example of such an image is shown in Fig. 2. It shows the contours of the Hall bar like the image in Fig. 1 due to the change in capacitance, when the tip traverses the Hall bar mesa. A dark feature can be seen close to the edge of the Hall bar (marked by the arrow), probably indicating a spot on the surface where additional charge has been deposited before.

When the tip is scanned above the surface at fixed U and fixed Δz, resistance images can be taken. This is the so-called scanning gate technique. The resistance images depend on the applied voltage U. We find that scanning with $U<-2$ V changes the sample characteristics permanently over time, probably because there are charge rearrangements in the doping plane or on the surface. All resistance images shown in this paper have therefore been taken at $U=-2$ V, where the sample was found to be sufficiently stable.

Figure 1 shows schematically between which voltage probes resistances are measured in parallel during each scan. These are two longitudinal resistances R_{xx1} and R_{xx2} and one of the Hall resistances R_{xy}. The second Hall resistance R'_{xy} can in principle be calculated from $R'_{xy}=R_{xy}+R_{xx1}-R_{xx2}$.

The dashed curves in Fig. 3 show the low frequency

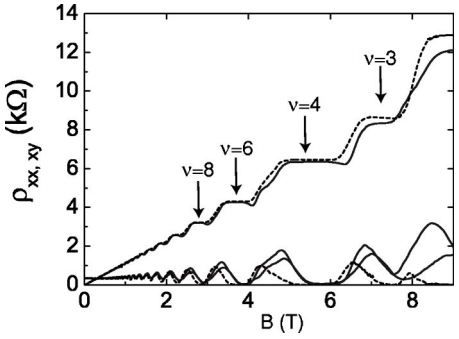

FIG. 3. Resistivity ρ_{xx} and ρ_{xy} of the 2DEG as a function of magnetic field. The measurements were taken at zero back gate voltage and at base temperature. The dashed curves were measured at a frequency of 20 Hz before any scan was performed. The solid lines are R_{xx1}, R_{xx2}, and R_{xy} measured after scanning induced sample changes have taken place. They are measured at a frequency of 624 Hz. Integer filling factors are indicated by arrows on the Hall trace.

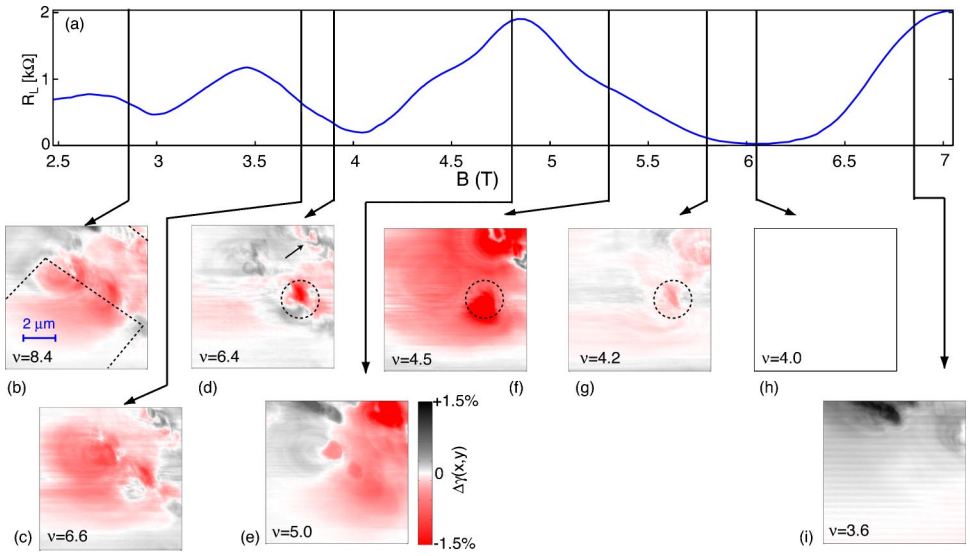

FIG. 4. (Color online) (a) Longitudinal resistance R_L measured in the absence of the scanning tip. Vertical lines indicate magnetic fields at which scanning gate images (b)–(i) were taken. (b)–(i) Scanning gate longitudinal resistance images taken at various magnetic field values indicated in (a). Images (g1) and (g2) are identical except that for (g2) the gray scale ranges from −0.5% to +0.5%, i.e., it is enhanced by a factor of 3. The corresponding filling factors for each image are indicated. The gray scale relates to the local tip-induced change of the relative backscattering strength $\Delta\gamma$ as discussed in the text. The measurements were taken at zero back gate voltage and at base temperature.

(20 Hz) longitudinal and Hall resistivities measured before any scan had been performed on the sample. Well developed Hall plateaus and minima in ρ_{xx} can be seen at integer filling factors. Scanning gate measurements were performed with lock-in technique at a frequency of 624 Hz with a time constant of 30 ms in order to achieve an acceptably high measurement bandwidth during scanning. The solid lines in Fig. 3 show the two longitudinal resistivities and the Hall resistance measured at this high frequency about one week later, i.e., after many scans with $U=-6$ V had been made. Causes for differences between the solid and the dashed curves are twofold: on the one hand, the higher measurement frequency together with the cable capacitances leads to small dips at the high field edge of the quantum Hall plateaus which can be well understood in an equivalent circuit model of the setup. On the other hand, repeated scanning at large negative U has modified the details of the ρ_{xx}-trace between integer filling factors and the overall density appears to be slightly increased. In fact, we found in earlier Kelvin probe studies[43] on two-dimensional electron gases that due to work function differences between the tip and the heterostructure materials and due to the spatially fixed doping and surface charges in the sample, a tip voltage of about $U=+0.5$ V is needed for minimizing the effect of the tip on the sample. This means that an applied voltage of $U=-2$ V corresponds to an effective voltage of −2.5 V acting on the electron gas. A huge number of images at a number of different tip voltages and magnetic fields have been taken within the course of a single cooldown. In the following, we present a selection of data taken at a tip-sample voltage of $U=-2$ V for which the sample was stable and scanned images were highly reproducible.

III. MEASUREMENT RESULTS AND DISCUSSION

Figure 4 shows longitudinal resistance data at various magnetic fields. The top trace [Fig. 4(a)] is the longitudinal resistance $R_L=R_{xx1}$ as a function of magnetic field B. Vertical lines indicate fields where scanned images of R_L were recorded. The respective arrows point to the corresponding images. The gray scale in these images will be explained below. Scanning a single image takes more than 2 h. Image (b) shows the boundaries of the Hall bar structure taken from a simultaneously recorded topography image (dotted line) for orientation.

The difficulty in presenting scanned R_L images is that this quantity varies over orders of magnitude as the magnetic field is changed. We have therefore plotted the data in terms of a different physically intuitive quantity, the relative backscattering amplitude γ. The introduction of this quantity allowed us to plot all resistance images in Fig. 4 using the same gray scale.

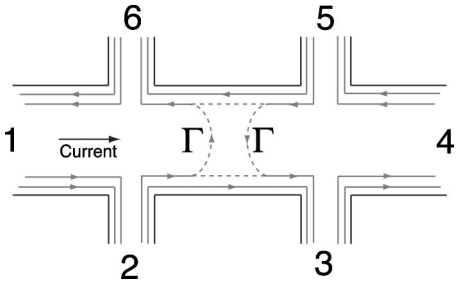

FIG. 5. Schematic representation of the Landauer-Büttiker description of the quantum Hall effect for the longitudinal resistance. Edge states are represented by solid lines with arrows. Γ is the backscattering probability between sample edges.

In order to introduce our data analysis and the quantity γ we consider the model situation depicted in Fig. 5 within the Landauer-Büttiker description.[9] The current is driven from contact 1 to 4 and the voltage is measured between contacts 3 and 2. Resistance arises due to backscattering in the region between these voltage probes. We therefore allow a certain local coupling Γ between the two edges of the sample, which may be mediated or altered by the tip induced potential. In this model, the longitudinal resistance is given by

$$R_L = R_{23,14} = \frac{h}{e^2 \nu} \frac{\gamma}{1-\gamma}. \tag{2}$$

Here, ν is the number of edge channels injected into the structure from the contacts. The function $\nu(B)$ will decrease with increasing magnetic field in a steplike manner, whenever the highest occupied Landau level becomes depopulated. The prefactor $h/e^2\nu$ represents the Hall resistance R_H in the absence of any scattering. The ratio $\gamma = \Gamma/\nu$ represents the relative backscattering strength between opposite edges of the Hall bar. If this quantity is zero, backscattering is absent and $R_L = 0$, if it is unity, all the edge channels injected from the contacts are fully backscattered and R_L diverges.

This view on R_L leads us to the following way to represent the data in terms of the empirical relative backscattering strength γ: We use the measured R_H as the empirically determined prefactor $h/e^2\nu$ in Eq. (2) and solve this equation for γ. This leads to

$$\gamma = \frac{R_L/R_H}{1 + R_L/R_H}.$$

This quantity is our empirical measure for the relative amount of backscattering between edges of the Hall bar sample. The advantage of using it for representing R_L-data is the fact that it maps resistances at different magnetic fields in the quantum Hall regime that can be different by orders of magnitude into the interval $\gamma \in [0,1]$.

The relative backscattering strength does also have a meaning in the semiclassical language of Drude transport. Straightforward analysis gives $\gamma = 1/(1 + W/L \tan \theta_H)$, where W/L is the width-to-length ratio of the structure and θ_H is the Hall angle. In this classical picture, a Hall angle of zero corresponds to $\gamma = 1$ while a Hall angle of $\pi/2$ corresponds to $\gamma = 0$.

In order to show that this quantity is meaningful in the experiment, we plot in Fig. 6 (solid line) raw R_L-R_H-data obtained from a magnetic field sweep in the absence of the scanning tip in the form of $\gamma(\nu)$, where ν represents the magnetic field converted into filling factor. The empirical parameter γ oscillates as a function of filling factor. At QHE minima of R_L also γ has its minimum, as expected. Maxima in γ occur at odd filling factors $\nu = 5, 7, 9$, where new spin degenerate Landau levels become occupied with increasing ν. For example, at $\nu = 5$ the third spin degenerate Landau level becomes occupied and at this maximum $\gamma \approx 0.22$, meaning that 22% of the incoming electrons are backscattered from one sample edge to the other.

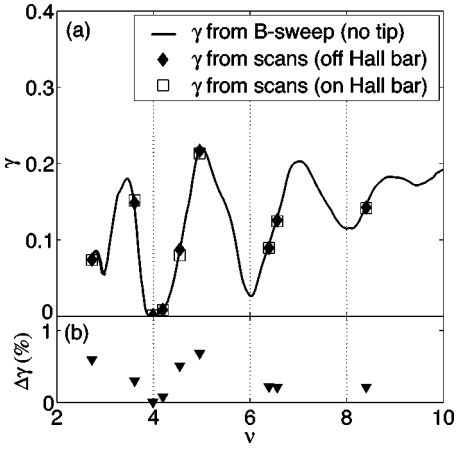

FIG. 6. (a) Relative backscattering probability γ in the quantum Hall regime as a function of filling factor ν. The solid line is determined from a magnetic field sweep in the absence of the scanning tip. The solid diamonds are average values of γ with the tip not scanning on the Hall bar mesa, open squares are the corresponding values with the tip on the mesa. (b) The filled triangles represent the average tip-induced changes $\Delta\gamma$.

In order to analyze the scanned images in the same fashion, we distinguish regions, where the tip scans on top of the Hall bar and others, where it does not. We first concentrate on spatially averaged properties of the images. The filled diamonds in Fig. 6(a) represent average resistance values as determined from regions in scanned resistance plots where the tip is not scanning on the Hall bar. This background resistance coincides with the magnetic field sweep data, as expected. The open squares in the figure correspond to average resistance values for the regions in scanned images where the tip is scanning over the Hall bar. It can be seen that the deviation of these values from the background resistance values (diamonds) is rather small indicating that *on average* the tip induced resistance change is small, typically below 1%, no matter at which filling factor it is determined.

The smallness of these tip induced changes allows us to determine the average tip-induced change in relative backscattering, $\Delta\gamma$, from

$$\Delta\gamma = \frac{\Delta(R_L/R_H)}{[1 + \langle R_L/R_H \rangle]^2},$$

where $\langle R_L/R_H \rangle$ is the longitudinal resistance at a given magnetic field normalized to the Hall resistance in the absence of the tip and $\Delta(R_L/R_H)$ is the spatially averaged root-mean-square deviation. The quantity $\Delta\gamma$ is shown in Fig. 6(b) as solid triangles. Of particular interest is $\Delta\gamma$ around filling factor 4. Exactly at this filling factor the tip-induced backscattering vanishes, while for filling factors slightly smaller or larger than 4, $\Delta\gamma$ takes on finite values up to almost 1%. These numbers reflect the fact that the image in Fig. 4(h) is completely featureless, while (f), (g), and (i) show an increasing corrugation with increasing value of $|\nu - 4|$. These results support the well accepted notion that at integer filling factors, states in the bulk of the Hall bar are completely localized. At $\nu = 4$ the local tip-induced perturbation is not

able to couple the extended edge states across this highly insulating region. At filling factors smaller or larger than 4, where states at the Fermi energy become increasingly extended and therefore couple the edges, the tip can also have an increasing effect on the interedge coupling.

Having discussed the averaged properties of the images shown in Figs. 4(f)–4(i), we now return to a more detailed discussion of their spatial structure. The first general remarkable feature is that the tip cannot only increase but also decrease the relative backscattering strength γ (bright vs dark regions in the images), i.e., $\Delta\gamma(x,y)$ can take positive and negative values. Certain local structures in the images tend to repeat when the filling factor is increased by about an integer multiple of 2, although the exact details may be different. An example is indicated with dashed circles in Figs. 4(d) and 4(g). At the same spot, structure can also be seen in (f). The particular feature marked in (d), (f), and (g) may be related with the charged spot observed in the measurement shown in Fig. 2. This overall local behavior reflects the $1/B$-periodicity of R_L on a local scale.

The structure of edge states seems to be important for the images as well. Local features in $\Delta\gamma$ line up along the edges of the Hall bar. This behavior can be seen in Figs. 4(b)–4(e). These measurements show the tendency that the features centered at edges become more localized with increasing B while structure in the bulk becomes less pronounced. Measurements at even lower fields (not shown) indicate that only at $\nu<10$, corresponding to $B>2.5$ T, features relate to the sample edges. This observation is in agreement with the general notion of the transition from the Shubnikov-de Haas regime, where localization is not important, to the quantum Hall regime, where the localization of states and the formation of extended edge states plays a crucial role.

The tip induced change in backscattering shows subtle capillary structures near the edges of the Hall bar, for example, as indicated by the arrow in Fig. 4(d) measured at filling factor $\nu=6.6$. The characteristic width of such capillaries can be as small as 200 nm. Similar structure has also been seen with a different local probe technique in Refs. 24 and 44. The minute details of these features depend very sensitively on magnetic field as seen from a comparison of Figs. 4(c) and 4(d). The origin of the structure, which may be due to an interplay of intrinsic disorder and tip-induced effects in our experiment, remains to be investigated in detail.

We proceed with a few brief and preliminary statements about scanning gate results for the Hall resistance R_{xy}. In general, we find that scanning in the interior of the sample between longitudinal voltage probes does not lead to a change in the Hall resistance at all. Furthermore, the Hall resistance can only be affected at magnetic fields where transitions between Hall plateaus occur. These resistance changes are bound to a region enclosed by the four leads forming the Hall cross. These observations are in agreement with the generally accepted concept of localized states in the bulk. They are also in agreement with the well-known observation that the plateau values of the Hall resistance are independent of sample characteristics and materials. In our experiment, the sample with the tip in different positions may be regarded as being equivalent to different samples. Constant R_{xy} values are observed on plateaus. In contrast, in the transition region between quantum Hall plateaus, the scanning gate images show an influence on the Hall resistance, when the tip is in the vicinity of the Hall cross. More detailed results on the Hall resistance have been obtained in a different set of experiments.[45]

IV. CONCLUSION

In this paper, we have reported scanning gate measurements on a Hall bar structure performed at 300 mK in the quantum Hall regime. Local features of the resistance images resemble the $1/B$-periodicity of the global longitudinal four-terminal resistance in the absence of the scanning tip. The appearance of features lining up along the sample edges corresponds to the formation of extended edge states and localized bulk states. Capillary fine structure on a submicron length scale indicate the intricate evolution of current carrying states at certain filling factors. Tip-induced Hall resistance changes are spatially bound to the region of the Hall cross and in magnetic field to transition regions between Hall plateaus.

*Electronic address: ihn@phys.ethz.ch

[1] K. von Klitzing, G. Dorda, and M. Pepper, Phys. Rev. Lett. **45**, 494 (1980).
[2] R. Prange and S. Girvin, *The Quantum Hall Effect* (Springer, New York, 1990).
[3] J. Hajdu, *Introduction to the Theory of the Integer Quantum Hall Effect* (Wiley-VCH, Weinheim, 1994).
[4] T. Chakraborty and P. Pietiläinen, *The Quantum Hall Effects: Integral and Fractional* (Springer, New York, 1995).
[5] B. Jeckelmann and B. Jeanneret, Rep. Prog. Phys. **64**, 1603 (2001).
[6] D. Chklovskii, B. Shklovskii, and L. Glazman, Phys. Rev. B **46**, 4026 (1992).
[7] M. Geller and G. Vignale, Physica B **212**, 283 (1995).
[8] M. Buttiker, Phys. Rev. B **38**, 9375 (1988).
[9] R. Haug, A. MacDonald, P. Streda, and K. von Klitzing, Phys. Rev. Lett. **61**, 2797 (1988).
[10] A. Kent, D. McKitterick, P. Hawker, and M. Henini, Helv. Phys. Acta **65**, 331 (1992).
[11] A. Shashkin, A. Kent, P. Harrison, L. Eaves, and M. Henini, Phys. Rev. B **49**, 5379 (1994).
[12] R. Knott, W. Dietsche, K. Klitzing, K. Eberl, and K. Ploog, Semicond. Sci. Technol. **10**, 117 (1995).
[13] R. van Haren, F. Blom, and J. Wolter, Phys. Rev. Lett. **74**, 1198 (1995).
[14] E. Yahel, D. Orgad, A. Palevski, and H. Shtrikman, Phys. Rev. Lett. **76**, 2149 (1996).
[15] E. Yahel, A. Tsukernik, A. Palevski, and H. Shtrikman, Phys. Rev. Lett. **81**, 5201 (1998).
[16] Y. Wei, J. Weis, K. Klitzing, and K. Eberl, Phys. Rev. Lett. **81**,

1674 (1998).
[17] A. Yacoby, H. Hess, T. Fulton, L. Pfeiffer, and K. West, Solid State Commun. **111**, 1 (1999).
[18] S. Ilani, J. Martin, E. Teitelbaum, J. Smet, D. Mahalu, V. Umansky, and A. Yacoby, Nature (London) **427**, 328 (2004).
[19] K. McCormick, M. Woodside, M. Huang, M. Wu, P. McEuen, C. Duruoz, and J. J. S. Harris, Phys. Rev. B **59**, 4654 (1999).
[20] P. Weitz, E. Ahlswede, J. Weis, K. Klitzing, and K. Eberl, Physica E (Amsterdam) **6**, 247 (2000).
[21] E. Ahlswede, P. Weitz, J. Weis, K. Klitzing, and K. Eberl, Physica B **298**, 562 (2001).
[22] E. Ahlswede, J. Weis, K. v. Klitzing, and K. Eberl, Physica E (Amsterdam) **12**, 165 (2002).
[23] G. Finkelstein, P. Glicofridis, S. Tessmer, R. Ashoori, and M. Melloch, Phys. Rev. B **61**, R16 323 (2000).
[24] G. Finkelstein, P. Glicofridis, R. Ashoori, and M. Shayegan, Science **289**, 90 (2000).
[25] G. Finkelstein, P. Glicofridis, S. Tessmer, R. Ashoori, and M. Melloch, Physica E (Amsterdam) **6**, 251 (2000).
[26] M. Woodside, C. Vale, P. McEuen, C. Kadow, K. Maranowski, and A. Gossard, Phys. Rev. B **64**, 041310 (2001).
[27] T. Ihn, J. Rychen, K. Ensslin, W. Wegscheider, and M. Bichler, Physica E (Amsterdam) **13**, 671 (2002).
[28] M. Eriksson, R. Beck, M. Topinka, J. Katine, R. Westervelt, K. Campman, and A. Gossard, Appl. Phys. Lett. **69**, 671 (1996).
[29] K. McCormick, M. Woodside, M. Huang, P. McEuen, C. Duruoz, and J. J. S. Harris, Physica B **249-251**, 79 (1998).
[30] R. Crook, C. Smith, M. Simmons, and D. Ritchie, J. Phys.: Condens. Matter **12**, L735 (2000).
[31] M. Topinka, B. LeRoy, R. Westervelt, S. Shaw, R. Fleischmann, E. Heller, K. Maranowski, and A. Gossard, Nature (London) **410**, 183 (2001).
[32] M. Woodside and P. McEuen, Science **296**, 1098 (2002).
[33] T. Ihn, J. Rychen, T. Cilento, K. Ensslin, W. Wegscheider, and M. Bichler, Physica E (Amsterdam) **12**, 691 (2002).
[34] R. Crook, C. Smith, A. Graham, I. Farrer, H. Beere, and D. Ritchie, Phys. Rev. Lett. **91**, 246803 (2003).
[35] A. Dorn, M. Peter, S. Kičin, T. Ihn, K. Ensslin, D. Driscoll, and A. Gossard, Appl. Phys. Lett. **82**, 2631 (2003).
[36] T. Ihn, *Electronic Quantum Transport in Mesoscopic Semiconductor Structures*, No. 192 in Springer Tracts in Modern Physics (Springer, New York, 2004).
[37] K. Karrai and R. Grober, Appl. Phys. Lett. **66**, 1842 (1995).
[38] H. Edwards, L. Taylor, W. Duncan, and A. Melmed, J. Appl. Phys. **82**, 980 (1997).
[39] J. Rychen, T. Ihn, P. Studerus, A. Herrmann, and K. Ensslin, Rev. Sci. Instrum. **70**, 2765 (1999).
[40] J. Rychen, T. Ihn, P. Studerus, A. Herrmann, and K. Ensslin, Rev. Sci. Instrum. **71**, 1695 (2000).
[41] J. Rychen, T. Ihn, P. Studerus, A. Herrmann, K. Ensslin, H. Hug, P. van Schendel, and H. Güntherodt, Appl. Surf. Sci. **157**, 290 (2000).
[42] R. Wiesendanger, *Scanning Probe Microscopy and Spectroscopy* (Cambridge University Press, Cambridge, 1994).
[43] T. Vančura, S. Kičin, T. Ihn, K. Ensslin, M. Bichler, and W. Wegscheider, Appl. Phys. Lett. **83**, 2602 (2003).
[44] S. Tessmer, P. Glicofridis, R. Ashoori, L. Levitov, and M. Melloch, Nature (London) **392**, 51 (1998).
[45] A. Baumgartner, T. Ihn, and K. Ensslin (unpublished).